bioRxiv preprint doi: https://doi.org/10.1101/2021.11.08.467797; this version posted November 8, 2021. The copyright holder for this preprint (which was not certified by peer review) is the author/funder, who has granted bioRxiv a license to display the preprint in perpetuity. It is made available under aCC-BY 4.0 International license.

1
The *Escherichia coli serS* gene promoter region overlaps with the *rarA* gene
2
3
4

5 **Kanika Jain[*], Tyler H. Stanage, Elizabeth A. Wood, and Michael M. Cox**

6 **Department of Biochemistry, University of Wisconsin-Madison, Madison, Wisconsin 53706**

7
8
9
10

11 ***Corresponding author**

12 **Email:** kjain5@wisc.edu

13
14
15
16
17
18
19
20

bioRxiv preprint doi: https://doi.org/10.1101/2021.11.08.467797; this version posted November 8, 2021. The copyright holder for this preprint (which was not certified by peer review) is the author/funder, who has granted bioRxiv a license to display the preprint in perpetuity. It is made available under aCC-BY 4.0 International license.

21 # Abstract

22 Deletion of the entire gene encoding the RarA protein of *Escherichia coli* results in a
23 growth defect and additional deficiencies that were initially ascribed to a lack of RarA function.
24 Further work revealed that most of the effects reflected the presence of sequences in the *rarA* gene
25 that affect expression of the downstream gene, *serS*. The *serS* gene encodes the seryl aminoacyl-
26 tRNA synthetase. Decreases in the expression of *serS* can trigger the stringent response. The
27 sequences that affect *serS* expression are located in the last 15 nucleotides of the *rarA* gene.

28

29 # Introduction

30

31 When a replication fork encounters roadblocks, such as DNA lesions, template strand breaks, or
32 DNA-bound proteins, it can stall. Outcomes may include fork collapse and replisome dissociation
33 (1-11). These events can have catastrophic consequences for genomic integrity and cell viability,
34 if left unrepaired. In bacteria, estimates vary, but replication forks may stall as often as once per
35 cell generation during normal growth conditions (2, 12-20). Most of the adverse replication fork
36 encounters are resolved using a variety of pathways that do not introduce mutations (2, 3, 7, 9-13,
37 21-26). Sometimes, a fork skips over the lesion and re-initiates downstream, leaving the lesion
38 behind in what is called as a post-replication gap (4, 8, 13, 27-31). There appear to be three major
39 paths for filling post-replication gaps in bacteria: (a) RecA-mediated homologous recombination
40 (32-35), (b) translesion DNA synthesis (1, 36, 37), and (c) a RecA-independent template switching
41 process (38-41).The *Escherichia coli* RarA protein is required for most of this RecA-independent
42 recombination (41). More prominently, the RarA protein is involved in the resolution of

bioRxiv preprint doi: https://doi.org/10.1101/2021.11.08.467797; this version posted November 8, 2021. The copyright holder for this preprint (which was not certified by peer review) is the author/funder, who has granted bioRxiv a license to display the preprint in perpetuity. It is made available under aCC-BY 4.0 International license.

43 recombination intermediates as part of an expanded RecFOR pathway for the amelioration of post-
44 replication gaps (*manuscript under review*).

45 The *Escherichia coli* RarA protein is an ATPase in the AAA+ superfamily (42, 43). The
46 *rarA* gene encodes a 447-amino-acid polypeptide with a predicted monomeric mass of 49594 kDa.
47 The protein is part of a highly conserved family. It is absent in archaea but highly conserved from
48 bacteria through eukaryotes, sharing about 40% identity and 56-58% similarity with its
49 *Saccharomyces cerevisiae* (Mgs1) and Homo sapiens (WRNIP1) homologs (42, 43). In *E. coli,*
50 RarA shares 25% amino acid identity with two other proteins: RuvB, a Holliday Junction helicase,
51 and DnaX, a subunit of DNA polymerase III replisome. DnaX encodes for Tau (τ) and Gamma (γ)
52 components of DNA polymerase III clamp loader complex, placing RarA in the clamp loader
53 AAA+ clade (42, 43).

54 In *E. coli* chromosome, the *rarA* gene is located at 20.21 centisomes (location
55 937,994>939,337). The *rarA* gene is immediately upstream of an essential gene, *serS*, a serine-
56 tRNA ligase, located at 20.24 centisomes. SerS is among the 20 aminoacyl-tRNA synthetases
57 (aaRSs) or tRNA-ligases present in the cell. aaRSs are the charging portals of tRNAs. They
58 generate a covalent linkage between an amino acid and its cognate tRNA to form an aminoacyl-
59 tRNA complex. The ribosome acts on this charged tRNA complex and transfers its attached amino
60 acid onto the growing peptide chain - thereby fostering the translation process in the cell. SerS
61 aminoacylates $tRNA^{Ser}$ and $tRNA^{Sec}$ with serine (44, 45). *serS* is mainly regulated by its promoter
62 (serSp1) with a transcription start located at $939{,}365^{th}$ position after the end of *rarA* gene (46)
63 (**Figure 1**).

bioRxiv preprint doi: https://doi.org/10.1101/2021.11.08.467797; this version posted November 8, 2021. The copyright holder for this preprint (which was not certified by peer review) is the author/funder, who has granted bioRxiv a license to display the preprint in perpetuity. It is made available under aCC-BY 4.0 International license.

64 **Figure 1: Identification of possible promoter/regulatory sequence of *serS* within the *rarA*
65 sequence.** Representation of predicted promoter sequences and their location in the last 40 amino
66 acids region of *rarA*.
67
68 aaRSs manage the growth and the stringent response in the cell by directly controlling the
69 two interdependent cellular processes: (1) the flux of protein synthesis, and (2) the levels of
70 uncharged tRNAs. The first process - the flux of protein synthesis - is directly dependent on the
71 amount of tRNA aminoacylated by aaRSs. Modifications in aaRSs production impedes cell growth
72 (47, 48). Globally, high levels of uncharged tRNA slow translation kinetics and thereby slow cell
73 growth - both in bacteria and eukaryotes (49-51). In bacteria, these high levels of uncharged tRNA
74 are detected by the (p)ppGpp synthetase -RelA- which in response induces a stringent response
75 and affects the cell growth (52-54).
76 SerS is notable as it is inhibited by serine hydroxamate, a small molecule often used by
77 investigators to induce the stringent response (55). We have found that the complete deletion of
78 the *rarA* gene slows cell growth, impedes SOS induction, and rescues DNA damage sensitivity of
79 several repair-deficient cells, effects we initially attributed to a lack of RarA function. This initial
80 conclusion was in error. All of these phenotypes disappear when a slightly more modest *rarA*
81 deletion is used that deletes more than 90% of the coding sequence, all but the last 41 codons. This
82 suggests that regulatory sequences that affect *serS* expression may be embedded in the *rarA* coding
83 sequence. Keeping a small portion of the *rarA* gene, that which encodes C-terminal of RarA, is
84 vital for optimal growth of the *E. coli* cell. A –35 segment of the *serS* promoter or some equivalent
85 regulatory sequence appears to be located in the last 15 nucleotides of the *rarA* gene.
86

bioRxiv preprint doi: https://doi.org/10.1101/2021.11.08.467797; this version posted November 8, 2021. The copyright holder for this preprint (which was not certified by peer review) is the author/funder, who has granted bioRxiv a license to display the preprint in perpetuity. It is made available under aCC-BY 4.0 International license.

87 # Materials and Methods:

88 ## Strain construction

89

90 All strains are *E. coli* MG1655 derivatives and are listed in **Table 1.** Some of the *rarA* strains
91 (*rarA*N406, *rarA*N430, *rarA*N437 and *rarA*N442) were made using *galK+* recombineering
92 method. *rarAΔN447* (EAW98) and all other strains were constructed using Lambda red
93 recombination as described by Datsenko and Wanner (59). Kanamycin resistance of these strains
94 was removed using FLP recombinase when required (62). All chromosomal mutations were
95 confirmed using Sanger sequencing. Standard transformation protocols were used to generate
96 strains harboring the indicated plasmids as listed in **Table 1**.

Strain	**Genotype**	**Parent strain**	**Source/Technique**
MG1655	*rarA+ recA+ exoI+ recJ+ recF+ recO+ recR+ polB+ dinB+ umuDC+*		George Weinstock
EAW98	*rarAΔN447* Kan+	MG1655	Lambda RED recombination
EAW974	*rarAΔN406*	MG1655	Gal K+ recombineering with no antibiotic markers
EAW968	*rarAΔN430*	MG1655	Gal K+ recombineering with no antibiotic markers
EAW1449	*rarAΔN437*	MG1655	Gal K+ recombineering with no antibiotic markers
EAW1450	*rarAΔN442*	MG1655	Gal K+ recombineering with no antibiotic markers
EAW629	Δ*recF*	MG1655	Transduction of MG1655 with P1 grown on ***ΔrecF***
EAW114	Δ*recO*	MG1655	Lambda RED recombination
EAW18	Δ*dinB*	MG1655	Lambda RED recombination
EAW573	Δ*recO rarAΔN447*	EAW98	Transduction of EAW98 with P1 grown on ***ΔrecO***

bioRxiv preprint doi: https://doi.org/10.1101/2021.11.08.467797; this version posted November 8, 2021. The copyright holder for this preprint (which was not certified by peer review) is the author/funder, who has granted bioRxiv a license to display the preprint in perpetuity. It is made available under aCC-BY 4.0 International license.

THS130	*ΔrecF rarAΔN447*	EAW98	Transduction of EAW98 with P1 grown on **Δ*recF***
THS13	*ΔdinB rarAΔN447*	EAW98	Transduction of EAW98 with P1 grown on **Δ*dinB***
EAW984	*ΔrecO rarAΔN406*	EAW974	Transduction of EAW974with P1 grown on **Δ*recO***
EAW989	*ΔrecF rarAΔN406*	EAW974	Transduction of EAW974 with P1 grown on **Δ*recF***
EAW979	*ΔdinB rarAΔN406*	EAW974	Transduction of EAW974 with P1 grown on **Δ*dinB***

97

98 **Table 1: List of strains used in this study**

99

100 Plasmid construction

101

102 All plasmids were sequenced to confirm the correct mutation(s)/insertion(s) following their
103 construction. pBAD-*serS* is a pBAD/myc-His A Nde + wt *serS.* pEAW1176 was constructed by
104 amplifying the wildtype *serS* gene containing NdeI and BamHI restriction cut sites from the *E.*
105 *coli* MG1655 genome in a PCR. pBAD/myc-His A Nde was cut with NdeI and BglII enzymes
106 (BglII creates compatible sticky ends with BamHI), while the PCR product was cut with NdeI and
107 BamHI enzymes. The PCR product was ligated into the pBAD/myc-His A. pEAW1012 is a
108 derivative of pRC7 plasmid (a lac+ mini-F low copy derivative of pFZY1) that expresses a WT
109 copy of the *rarA* gene.

110

111 Growth curve

112 Overnight cultures of indicated strains were diluted 1:100 in LB medium. 100 µl of each culture
113 was poured in a clear bottom 96 well plate (Corning). Cultures were grown at 37° C with orbital

bioRxiv preprint doi: https://doi.org/10.1101/2021.11.08.467797; this version posted November 8, 2021. The copyright holder for this preprint (which was not certified by peer review) is the author/funder, who has granted bioRxiv a license to display the preprint in perpetuity. It is made available under aCC-BY 4.0 International license.

114 shaking in a BioTek Synergy 2 plate reader. OD_{600} values were taken every 10 minutes for over
115 the course of 800 minutes. OD_{600} values were normalized by subtracting out the OD_{600} value of
116 only LB media. All growth curves represent averaged values from the three biological replicate
117 experiments.
118

119 Growth competition assays

120 Growth competition assays were conducted as previously described (63) using a method originally
121 described by Lenski (60). The Δ*araBAD* ΔParaB marker was included on either wild type
122 (MG1655) or mutant (Δ*rarA*) in separate experiments to control for any effect the marker may
123 have had on cell fitness.
124

125 Drug sensitivity assay

126 Overnight cultures of indicated strains were diluted 1:100 in fresh LB medium. Cultures were
127 grown at 37°C with aeration and shaking until the OD_{600} measured 0.2. 1 mL aliquots were taken
128 from each culture and were serially diluted in 1X PBS buffer (137 mM NaCl, 2.7 mM KCl, 10
129 mM Na_2HPO_4, 1.8 mM KH_2PO_4, 1 mM $CaCl_2$ and 0.5 mM $MgCl_2$) to 10^{-6}. 10 µL of each dilution
130 were spot plated on LB agar plates containing the indicated media. Plates were incubated overnight
131 at 37°C and imaged the following day using a FOTO/Analyst Apprentice Digital Camera System
132 (Fotodyne, Inc.). All experiments were conducted at least three times.
133

134 SOS induction assay

bioRxiv preprint doi: https://doi.org/10.1101/2021.11.08.467797; this version posted November 8, 2021. The copyright holder for this preprint (which was not certified by peer review) is the author/funder, who has granted bioRxiv a license to display the preprint in perpetuity. It is made available under aCC-BY 4.0 International license.

135 Plasmid expressing the Green Fluorescent Protein (GFP) under the regulation of *recN* promoter
136 (pEAW903) was used in this assay. First, either empty vector (pQBi63) or pEAW903 was
137 transformed into the appropriate strains (WT, *rarA*ΔN447, or *rarAΔN406*) and the transformants
138 were selected on Amp100 (100 µg/ml) plates. The transformants were then grown in 3ml of LB +
139 Amp100 medium overnight at 37°C. The next day, the cultures were diluted in 1:1000 ratio in LB
140 + Amp100 broth and 150µl of sample were poured into each well of a 96-well plate (Corning
141 Incorporated/Costar) and put into the plate reader (Synergy H1 Hybrid Reader by BioTek). The
142 samples were allowed to grow for 1000 mins at 37°C, with OD_{600} and GFP fluorescence
143 (488/515nm) recorded at every 10 minutes. Relative fluorescence was calculated by normalizing
144 the fluorescence reading to the OD_{600} of the culture.

145 Analysis of cell shape: Bright field microscopy

146 All cells were grown overnight at 37°C and the saturated culture diluted in 1:100 ratio and grown
147 in LB media till O.D. reaches 1.0. 200 µL of culture were then pelleted down, resuspended in
148 1XPBS buffer and incubated with 2 µl of FM-64 dye (0.33M) on ice for at least 30 mins. For
149 imaging, 2µl of this mixture were loaded onto 0.16mm thick borosilicate glass made coverslips
150 (Azer scientific) and sandwiched with 1% agarose gel pad. For all measurements of cell size and
151 filamentation, wide-field microscopy was conducted on a STORM/TIRF inverted microscope
152 ECLIPSE Ti-E (Nikon) (100× objective). Images using DIA and dsRed filters were collected on
153 an ORCA Flash 4.0 Hamamatsu camera. A bright-field and dsRed image (at 100 ms and 50ms
154 exposure respectively) were taken at multiple fields of view to determine the cell shape and length.
155 For analysis, all images were imported into MicrobeJ, an ImageJ plugin, to outline cells. Selected

bioRxiv preprint doi: https://doi.org/10.1101/2021.11.08.467797; this version posted November 8, 2021. The copyright holder for this preprint (which was not certified by peer review) is the author/funder, who has granted bioRxiv a license to display the preprint in perpetuity. It is made available under aCC-BY 4.0 International license.

156 cells were manually filtered for any outliers. All strains were imaged in triplicates and the cell size
157 of each strain is averaged compiling each repeat.

158 Results

159 It is well documented that RarA is involved in the maintenance of genome stability in cells, but its
160 precise function and mechanism of action remains an enigma. To identify the phenotypic
161 contribution of RarA in cells, we created a MG1655 derivative carrying a full deletion of the *rarA*
162 allele. No growth or viability phenotype has previously been ascribed to strains with a *rarA* gene
163 deletion (42, 43, 56-58). Previous work has focused on a modified *rarA* gene in which a
164 chloramphenicol cassette has replaced either the first 600 nucleotides of the *rarA* gene (42, 43, 56,
165 57) or codons 113-349 (58), both in an *E. coli* AB1157 background. As most of our constructs are
166 based on *E. coli* strain MG1655, we constructed a complete *rarA* gene deletion in the MG1655
167 background using Datsenko and Wanner method (59) (**Figure 2A**), and then studied the effect of
168 this deletion on cell fitness.

169 Complete deletion of *rarA* causes a growth defect and reduced cell 170 size of MG1655 *E. coli* cells

171 Using a plate reader, we noted and compared the growth of the *rarA*Δ*N447*strain to wild type cells
172 at 37°C every 10 mins for 18hrs. The *rarA*Δ*N447* cells grew more slowly than wild type cells.
173 (**Figure 2B**). To document the growth defect of the *rarA*Δ*N447* mutant with a different and more
174 sensitive method, we carried out a direct competition assay between the wild type strain and the
175 *rarA*Δ*N447*strain, using an approach developed by Lenski and colleagues (60). (**Figure 2C**). Wild

bioRxiv preprint doi: https://doi.org/10.1101/2021.11.08.467797; this version posted November 8, 2021. The copyright holder for this preprint (which was not certified by peer review) is the author/funder, who has granted bioRxiv a license to display the preprint in perpetuity. It is made available under aCC-BY 4.0 International license.

176 type or mutant cells were modified to carry a neutral Ara– mutation (which confers a red color on
177 colonies when grown on tetrazolium arabinose (TA) indicator plates) to permit color-based scoring
178 of mixed populations. Overnight cultures of the *rarAΔN447*strain were mixed in a 50/50 ratio with
179 isogenic wild type cells carrying the Ara– mutation, or vice versa. The mixed culture was then
180 diluted and grown up again on successive days, with plating to count red and white colonies
181 occurring once each day. Earlier work (60, 61) demonstrated that the Ara– mutation does not affect
182 growth rates by itself. We found that the wild type cells outgrew the *rarAΔN447* cells and
183 dominated the mixed cultures almost completely within 24 hours (**Figure 2C**). We further
184 investigated the phenotypic dissimilarities between *rarAΔN447* and WT cells using bright field
185 microscopy. We observed that *rarAΔN447* cells were substantially smaller than *rarA*+ cells
186 (1.58μm [SEM =0.01] versus 2μm [SEM = 0.01] in length) (**Figure 2D**). RarA is well documented
187 as a vital player in the DNA recombination and repair process. Suppressing the DNA repair system
188 exerts stress response in the cell. With the data collected above, we presumed that the complete
189 deletion of *rarA* impedes the damage tolerance capability of the cells that results in a significant
190 growth impact.

191 Phenotypic defects of Δ*rarA* cells are attributed to the lower 192 expression of *serS* gene

193 For further affirmation of the results obtained above, we performed a complementation test. The
194 pRC7 plasmid carrying a wild type copy of *rarA* along with ampicillin marker is employed in this
195 study. We incorporated this plasmid into *rarAΔN447* cell and test its growth rate. Surprisingly, we
196 observed no rescue of the growth defect even in the presence of wild-type copy of *rarA* on the
197 plasmid (**Figure 2E**). This observation signals that the growth defect observed earlier is not

bioRxiv preprint doi: https://doi.org/10.1101/2021.11.08.467797; this version posted November 8, 2021. The copyright holder for this preprint (which was not certified by peer review) is the author/funder, who has granted bioRxiv a license to display the preprint in perpetuity. It is made available under aCC-BY 4.0 International license.

198 directly associated with the absence of *rarA* but might be an outcome of that deletion on other
199 growth-related genes.

200 Based on the genomic location position of *rarA*, we hypothesized that the growth defect might be
201 ascribed to the defect in the closest downstream essential gene - *serS*. It is well documented that
202 the addition of SHX (serine hydroxamate), an inhibitor of the *serRS* gene, causes growth defects
203 in *E. coli* cells even under the nutrient rich conditions (55). Changes in the levels of *serS* are
204 expected to fluctuate the levels of charged to uncharged tRNA ratios and thereby the cell growth.
205 Decreased cell viability of *rarAΔN447* could be a result of the decreased *serS* levels in the cell. To
206 test this hypothesis, we incorporated a plasmid overexpressing *serS* in *rarAΔN447* cells.
207 Overproduction of *serS* rescued the growth defect of *rarAΔN447* cells (**Figure 2F**). This result
208 signals the presence of promoter element/regulatory sequence for *serS* gene within the coding
209 region of a *rarA* gene. Removal of that segment impacts the level of *serS* in the cell.

210 **Figure 2: Complete deletion of *rarA (rarAΔN447)* causes a growth defect in *E. coli* cell.**
211 (A) Schematic of a complete deletion of *rarA* via a FLP recombinase method in *E. coli*
212 chromosome. The *rarA* gene segment is replaced by a Kan cassette. (B) Growth curve: Deletion
213 of complete *rarA* gene exhibit growth defect. (C) Growth competition: *rarAΔN447* is outcompeted
214 by WT cells (D) Average cell size of Δ*rarA* cells decreases compared to WT cells. (E) Addition
215 of pRC7-*rarA*, carrying WT *rarA* copy, in Δ*rarA* cell does not rescue its growth defect. (F)
216 Overexpression of *serS* using pBAD vector rescues the growth defect of Δ*rarA* cells (blue line).

217

bioRxiv preprint doi: https://doi.org/10.1101/2021.11.08.467797; this version posted November 8, 2021. The copyright holder for this preprint (which was not certified by peer review) is the author/funder, who has granted bioRxiv a license to display the preprint in perpetuity. It is made available under aCC-BY 4.0 International license.

218 Using the multi-genome browser of Ecocyc, we next searched for the orthologs of *rarA* in a broad
219 range of organisms and then mapped the extent to which those orthologs have maintained their
220 genetic context relative to *E. coli.* It revealed that the positioning of the *serS* gene - right
221 downstream of the *rarA* gene locus - exists only in γ-proteobacteria class of the Proteobacteria
222 phylum (**Figure 3**). Conservation of this proximity between *rarA* and *serS* genes across this class
223 indicates their possible interconnection in other organisms of this class as well.

224 **Figure 3: Multiple genome sequence alignment to identify orthologs of *rarA*, and the**
225 **conservation of its genetic context in other organisms.**

226

227 Identification of promoter/regulatory sequence for *serS* gene in *rarA* 228 sequence

229 We next aimed to identify the segment within a *rarA* gene that is controlling the *serS* expression
230 under normal conditions. We constructed various *rarA* mutations differing in the number of
231 nucleotides deleted from the N- terminus of the *rarA* to figure out the minimum region of *rarA*
232 required to remain intact to mitigate the growth defect of *rarA*Δ*N447* cells. GalK+ recombineering
233 method instead of Datensko Warner method was used to avoid any effect of kanamycin cassette
234 sequence on the *serS* expression. We created four variants - *rarA*Δ*N406*, *rarA*Δ*N430*, *rarA*Δ*N437*,
235 and *rarA*Δ*N442*, and studied their growth and cell morphology profiles (**Figure 4A).** Interestingly,
236 none of these mutants showed any growth adversity like *rarA*Δ*N447* (**Figure 4B and 4C**).
237 However, the creation of complete deletion of *rarA* via galK recombineering method failed. This
238 indicates that there exists a possible promoter or regulatory sequence for *serS* within the last 5

bioRxiv preprint doi: https://doi.org/10.1101/2021.11.08.467797; this version posted November 8, 2021. The copyright holder for this preprint (which was not certified by peer review) is the author/funder, who has granted bioRxiv a license to display the preprint in perpetuity. It is made available under aCC-BY 4.0 International license.

239 codons of *rarA* – deletion of which hampers the *serS* expression and thereby the growth of the cell.
240 *serS* is mainly regulated by its promoter (serSp1) with a transcription start located at 28 nucleotides
241 downstream from the end of *rarA* gene (46). Tracing back its possible promoter region, we
242 suspected that the –10 region for this serSp1 is located at ~14 nucleotide from the *rarA* end and its
243 –35 is located (although there is no good consensus –35 there) within the last ~15 nucleotides of
244 *rarA* gene. A –35 segment of the *serS* promoter or some equivalent regulatory sequence within
245 this last segment of *rarA* gene makes the complete deletion of *rarA* an infeasible option in the *E.*
246 *coli* cell.
247
248 **Figure 4: Analysis of the effect of various *rarA* deletion (*rarA∆N406, rarA∆N430, rarA∆N437,*
249 *rarA∆N442, and rarA∆N447*) on the growth and cell size.**
250 (A) Schematic of *rarA* gene, highlighting the possible promoter regions and positions of different
251 deletions made. (B) Growth curve: ∆*rarAN406*, ∆*rarAN430*, ∆*rarAN437,* ∆*rarAN442* does not
252 exhibit a growth defect (C) Cell size: *rarA∆N406*, *rarA∆N430*, *rarA∆N437, rarA∆N442* has cell
253 morphology comparable to WT.
254

255 Consequences of ∆*rarA* on damage sensitivity of cells compromised 256 with other DNA repair system

257 We tested the drug sensitivity of ∆*rarA447* cell alone and it in combination with other repair
258 systems. The absence of a complete *rarA* sequence itself does not increase the cell sensitivity to
259 DNA damaging agents like UV or NFZ. Removal of a RecA-loading system like RecF or RecO,
260 however, increases the sensitivity to almost all kinds of damages. Interestingly, deletion of *rarA*
261 in *recF* or *recO* background rescues their damage sensitivity. Complete deletion of *rarA* in ∆*pol*

bioRxiv preprint doi: https://doi.org/10.1101/2021.11.08.467797; this version posted November 8, 2021. The copyright holder for this preprint (which was not certified by peer review) is the author/funder, who has granted bioRxiv a license to display the preprint in perpetuity. It is made available under aCC-BY 4.0 International license.

262 *IV* background also decreases the sensitivity of *pol IV*- cells to both UV and NFZ induced damages
263 *(***Supplementary fig. 1)**. Moreover, we observed that SOS response is also induced in *rarA*ΔN447,
264 at both with and without external damaging conditions (UV treatment). The induction was much
265 higher than a WT cell *(***Supplementary fig. 2)**. Interestingly, none of these results were replicated
266 when Δ*rarA*N406 background was used instead of *rarA*ΔN447.
267
268 With all these observations, we confirmed that the phenotype due to the complete deletion of *rarA*
269 is attributed to the decreased levels of *serS* in the cell. Decreased level of *serS* could cause a
270 stringent response which activates the level of ppGpp. High levels of ppGpp act by rescuing the
271 stalled RNA polymerases. The rescue of Δ*pol IV/* Δ*recF/* Δ*recO* cells' drug sensitivity on deletion
272 of *rarA*ΔN447 may be due to the rescue of stalled RNA polymerases, an outcome of the action of
273 high levels of ppGpp in *rarA*ΔN447 cells. High SOS levels could also be a repercussion of this
274 same phenomenon. Deletion of all but the last 41 codons of *rarA* eliminates all these phenotypes.
275

276 Discussion

277 The major conclusion of this work is straightforward. Genetic elements affecting the expression
278 of the *serS* gene are embedded in the final five codons of the upstream *rarA* gene. Upon complete
279 deletion of *rarA*, we had documented a variety of phenotypic effects (supplementary data) that we
280 initially attributed to a loss of *rarA* function. These disappeared when we made use of *rarA*
281 deletions that encompasses most but not all of the gene. We now attribute the effects to changes
282 in *serS* expression, possibly reflecting some aspect of a stringent response.

bioRxiv preprint doi: https://doi.org/10.1101/2021.11.08.467797; this version posted November 8, 2021. The copyright holder for this preprint (which was not certified by peer review) is the author/funder, who has granted bioRxiv a license to display the preprint in perpetuity. It is made available under aCC-BY 4.0 International license.

283 The *serS* promoter element that is within the *rarA* gene has not been identified. The region
284 in question is positioned so as to potentially include a –35 region for the promoter. However, no –
285 35 consensus is evident.
286
287

288 # References

289
290 1. Cox MM, Goodman MF, Kreuzer KN, Sherratt DJ, Sandler SJ, Marians KJ. The
291 importance of repairing stalled replication forks. Nature. 2000;404(6773):37-41.
292 2. Cox MM. Recombinational DNA repair of damaged replication forks in *Escherichia coli*:
293 questions. Annual Review of Genetics. 2001;35:53-82.
294 3. Kowalczykowski SC. Initiation of genetic recombination and recombination-dependent
295 replication. Trends in Biochemical Sciences. 2000;25:156-65.
296 4. Kuzminov A. Recombinational repair of DNA damage in *Escherichia coli* and
297 bacteriophage lambda. Microbiology & Molecular Biology Reviews. 1999;63(4):751-813.
298 5. Kuzminov A. Single-strand interruptions in replicating chromosomes cause double-strand
299 breaks. Proceedings of the National Academy of Sciences of the United States of America.
300 2001;98(15):8241-6.
301 6. Michel B. Replication fork arrest and DNA recombination. Trends in Biochemical
302 Sciences. 2000;25:173-8.
303 7. Michel B, Boubakri H, Baharoglu Z, LeMasson M, Lestini R. Recombination proteins and
304 rescue of arrested replication forks. DNA Repair. 2007;6(7):967-80.
305 8. Heller RC, Marians KJ. Replisome assembly and the direct restart of stalled replication
306 forks. Nature Reviews Molecular Cell Biology. 2006;7(12):932-43.
307 9. Klein HL, Kreuzer KN. Replication, recombination, and repair: going for the gold.
308 Molecular Cell. 2002;9(3):471-80.
309 10. Lopes M, Cotta-Ramusino C, Pellicioli A, Liberi G, Plevani P, Muzi-Falconi M, et al. The
310 DNA replication checkpoint response stabilizes stalled replication forks. Nature.
311 2001;412(6846):557-61.
312 11. Merrikh H, Zhang Y, Grossman AD, Wang JD. Replication-transcription conflicts in
313 bacteria. Nature Reviews Microbiology. 2012;10(7):449-58.
314 12. Cox MM. Recombinational DNA repair in bacteria and the RecA protein. Progress in
315 Nucleic Acids Research and Molecular Biology. 2000;63:311-66.
316 13. Cox MM. The nonmutagenic repair of broken replication forks via recombination.
317 Mutation Research-Fundamental and Molecular Mechanisms of Mutagenesis. 2002;510(1-2
318 Special Issue SI):107-20.
319 14. Kuzminov A. Collapse and repair of replication forks in *Escherichia coli*. Molecular
320 Microbiology. 1995;16(3):373-84.
321 15. McCool JD, Long E, Petrosino JF, Sandler HA, Rosenberg SM, Sandler SJ. Measurement
322 of SOS expression in individual *Escherichia coli* K-12 cells using fluorescence microscopy.
323 Molecular Microbiology. 2004;53(5):1343-57.

bioRxiv preprint doi: https://doi.org/10.1101/2021.11.08.467797; this version posted November 8, 2021. The copyright holder for this preprint (which was not certified by peer review) is the author/funder, who has granted bioRxiv a license to display the preprint in perpetuity. It is made available under aCC-BY 4.0 International license.

324 16. Michel B, Flores MJ, Viguera E, Grompone G, Seigneur M, Bidnenko V. Rescue of
325 arrested replication forks by homologous recombination. Proceedings of the National Academy of
326 Sciences of the United States of America. 2001;98(15):8181-8.
327 17. Michel B, Grompone G, Flores MJ, Bidnenko V. Multiple pathways process stalled
328 replication forks. Proceedings of the National Academy of Sciences of the United States of
329 America. 2004;101(35):12783-8.
330 18. Syeda AH, Hawkins M, McGlynn P. Recombination and Replication. Cold Spring Harbor
331 Perspectives in Biology. 2014;6(11).
332 19. Mangiameli SM, Veit BT, Merrikh H, Wiggins PA. The Replisomes Remain Spatially
333 Proximal throughout the Cell Cycle in Bacteria. PLoS Genetics. 2017;13(1):e006582.
334 20. Courcelle J, Wendel BM, Livingstone DD, Courcelle CT. RecBCD is required to complete
335 chromosomal replication: Implications for double-strand break frequencies and repair
336 mechanisms. DNA Repair. 2015;32:86-95.
337 21. Kuzminov A. DNA replication meets genetic exchange: Chromosomal damage and its
338 repair by homologous recombination. Proceedings of the National Academy of Sciences of the
339 United States of America. 2001;98(15):8461-8.
340 22. Kuzminov A, Stahl FW. Double-strand end repair via the RecBC pathway in *Escherichia*
341 *coli* primes DNA replication. Genes & Development. 1999;13(3):345-56.
342 23. Michel B, Recchia GD, Penel-Colin M, Ehrlich SD, Sherratt DJ. Resolution of Holliday
343 junctions by RuvABC prevents dimer formation in rep mutants and UV-irradiated cells. Molecular
344 Microbiology. 2000;37(1):180-91.
345 24. Heller RC, Marians KJ. Replication fork reactivation downstream of a blocked nascent
346 leading strand. Nature. 2006;439(7076):557-62.
347 25. Mirkin EV, Mirkin SM. Replication fork stalling at natural impediments. Microbiology
348 and Molecular Biology Reviews. 2007;71(1):13-35.
349 26. Aguilera A, Garcia-Muse T. Causes of genome instability. Annual Review of Genetics,
350 Vol 47. 2013;47:1-32.
351 27. Branzei D, Szakal B. Building up and breaking down: mechanisms controlling
352 recombination during replication. Critical Reviews in Biochemistry and Molecular Biology.
353 2017;52(4):381-94.
354 28. Rothman RH, Clark AJ. Defective excision and postreplication repair of UV-damaged
355 DNA in a recL mutant strain of *E. coli* K-12. Molecular & General Genetics. 1977;155(3):267-77.
356 29. Goodman MF. The discovery of error-prone DNA polymerase V and its unique regulation
357 by RecA and ATP. J Biol Chem. 2014;289(39):26772-82.
358 30. Umezu K, Chi NW, Kolodner RD. Biochemical interaction of the *Escherichia coli* RecF,
359 RecO, and RecR proteins with RecA protein and single-stranded DNA binding protein. Proc Natl
360 Acad Sci U S A. 1993;90(9):3875-9.
361 31. Umezu K, Kolodner RD. Protein interactions in genetic recombination in *Escherichia coli*.
362 Interactions involving RecO and RecR overcome the inhibition of RecA by single-stranded DNA-
363 binding protein. J Biol Chem. 1994;269(47):30005-13.
364 32. Bork JM, Cox MM, Inman RB. The RecOR proteins modulate RecA protein function at 5
365 ' ends of single-stranded DNA. EMBO Journal. 2001;20(24):7313-22.
366 33. Fuchs RP. Tolerance of lesions in *E. coli*: Chronological competition between translesion
367 synthesis and damage avoidance. DNA Repair. 2016;44:51-8.
368 34. Grompone G, Sanchez N, Ehrlich SD, Michel B. Requirement for RecFOR-mediated
369 recombination in priA mutant. Molecular Microbiology. 2004;52(2):551-62.

bioRxiv preprint doi: https://doi.org/10.1101/2021.11.08.467797; this version posted November 8, 2021. The copyright holder for this preprint (which was not certified by peer review) is the author/funder, who has granted bioRxiv a license to display the preprint in perpetuity. It is made available under aCC-BY 4.0 International license.

370 35. Kuzminov A. RuvA, RuvB and RuvC proteins: cleaning-up after recombinational repairs
371 in *E. coli*. . Bioessays. 1993;15(5):355-8.
372 36. Henrikus SS, van Oijen AM, Robinson A. Specialised DNA polymerases in *Escherichia*
373 *coli*: roles within multiple pathways. Current Genetics. 2018;64(6):1189-96.
374 37. Bichara M, Meier M, Wagner J, Cordonnier A, Lambert IB. Postreplication repair
375 mechanisms in the presence of DNA adducts in *Escherichia coli*. Mutation Research-Reviews in
376 Mutation Research. 2011;727(3):104-22.
377 38. Dutra BE, Sutera VA, Jr., Lovett ST. RecA-independent recombination is efficient but
378 limited by exonucleases. Proc Natl Acad Sci U S A. 2007;104(1):216-21.
379 39. Lovett ST, Hurley RL, Sutera VA, Aubuchon RH, Lebedeva MA. Crossing over between
380 regions of limited homology in *Escherichia coli*: RecA-dependent and RecA-independent
381 pathways. Genetics. 2002;160(3):851-9.
382 40. Lovett ST. Template-switching during replication fork repair in bacteria. DNA Repair.
383 2017;56:118-28.
384 41. Jain K, Wood EA, Romero ZJ, Cox MM. RecA-independent recombination: Dependence
385 on the Escherichia coli RarA protein. Mol Microbiol. 2021;115(6):1122-37.
386 42. Sherratt DJ, Soballe B, Barre FX, Filipe S, Lau I, Massey T, et al. Recombination and
387 chromosome segregation. Philosophical Transactions of the Royal Society of London Series B-
388 Biological Sciences. 2004;359(1441):61-9.
389 43. Barre FX, Soballe B, Michel B, Aroyo M, Robertson M, Sherratt D. Circles: The
390 replication-recombination-chromosome segregation connection. Proceedings of the National
391 Academy of Sciences of the United States of America. 2001;98(15):8189-95.
392 44. Leinfelder W, Zehelein E, Mandrand-Berthelot MA, Böck A. Gene for a novel tRNA
393 species that accepts L-serine and cotranslationally inserts selenocysteine. Nature.
394 1988;331(6158):723-5.
395 45. Baron C, Böck A. The length of the aminoacyl-acceptor stem of the selenocysteine-specific
396 tRNA(Sec) of Escherichia coli is the determinant for binding to elongation factors SELB or Tu. J
397 Biol Chem. 1991;266(30):20375-9.
398 46. Keseler IM, Collado-Vides J, Santos-Zavaleta A, Peralta-Gil M, Gama-Castro S, Muñiz-
399 Rascado L, et al. EcoCyc: a comprehensive database of Escherichia coli biology. Nucleic Acids
400 Res. 2011;39(Database issue):D583-90.
401 47. Bremer H, Dennis PP. Modulation of Chemical Composition and Other Parameters of the
402 Cell at Different Exponential Growth Rates. EcoSal Plus. 2008;3(1).
403 48. Dai X, Zhu M, Warren M, Balakrishnan R, Patsalo V, Okano H, et al. Reduction of
404 translating ribosomes enables Escherichia coli to maintain elongation rates during slow growth.
405 Nat Microbiol. 2016;2:16231.
406 49. Hinnebusch AG. TRANSLATIONAL REGULATION OF GCN4 AND THE GENERAL
407 AMINO ACID CONTROL OF YEAST. Annual Review of Microbiology. 2005;59(1):407-50.
408 50. Potrykus K, Cashel M. (p)ppGpp: Still Magical? Annual Review of Microbiology.
409 2008;62(1):35-51.
410 51. Srivatsan A, Wang JD. Control of bacterial transcription, translation and replication by (p)
411 ppGpp. Current Opinion in Microbiology. 2008;11(2):100-5.
412 52. Gourse RL, Chen AY, Gopalkrishnan S, Sanchez-Vazquez P, Myers A, Ross W.
413 Transcriptional Responses to ppGpp and DksA. Annual Review of Microbiology. 2018;72(1):163-
414 84.

bioRxiv preprint doi: https://doi.org/10.1101/2021.11.08.467797; this version posted November 8, 2021. The copyright holder for this preprint (which was not certified by peer review) is the author/funder, who has granted bioRxiv a license to display the preprint in perpetuity. It is made available under aCC-BY 4.0 International license.

415 53. Hauryliuk V, Atkinson GC, Murakami KS, Tenson T, Gerdes K. Recent functional insights
416 into the role of (p)ppGpp in bacterial physiology. Nature Reviews Microbiology. 2015;13(5):298-
417 309.
418 54. Liu KQ, Bittner AN, Wang JD. Diversity in (p)ppGpp metabolism and effectors. Current
419 Opinion in Microbiology. 2015;24:72-9.
420 55. Tosa T, Pizer Lewis I. Effect of Serine Hydroxamate on the Growth of Escherichia coli.
421 Journal of Bacteriology. 1971;106(3):966-71.
422 56. Lestini R, Michel B. UvrD controls the access of recombination proteins to blocked
423 replication forks. EMBO J. 2007;26(16):3804-14.
424 57. Michel B, Sinha AK. The inactivation of rfaP, rarA or sspA gene improves the viability of
425 the *Escherichia coli* DNA polymerase III holD mutant. Molecular Microbiology. 2017;in process.
426 58. Shibata T, Hishida T, Kubota Y, Han YW, Iwasaki H, Shinagawa H. Functional overlap
427 between RecA and MgsA (RarA) in the rescue of stalled replication forks in *Escherichia coli*.
428 Genes to Cells. 2005;10(3):181-91.
429 59. Datsenko KA, Wanner BL. One-step inactivation of chromosomal genes in *Escherichia*
430 *coli* K-12 using PCR products. Proceedings of the National Academy of Sciences of the United
431 States of America. 2000;97(12):6640-5.
432 60. Lenski RE. Quantifying fitness and gene stability in microorganisms. Biotechnology.
433 1991;15:173-92.
434 61. Byrne RT, Chen SH, Wood EA, Cabot EL, Cox MM. Surviving extreme exposure to
435 ionizing radiation: *Escherichia coli* genes and pathways
436 . Journal of Bacteriology. 2014;196:3534-45.
437 62. Huang LC, Wood EA, Cox MM. Convenient and reversible site-specific targeting of
438 exogenous DNA into a bacterial chromosome by use of the FLP recombinase: the FLIRT system.
439 Journal of Bacteriology. 1997;179(19):6076-83.
440 63. Kim T, Chitteni-Pattu S, Cox BL, Wood EA, Sandler SJ, Cox MM. Directed evolution of
441 RecA variants with enhanced capacity for conjugational recombination. PLoS Genet.
442 2015;11(6):e1005278.
443

444

445 # Supporting information

446 **Supplementary Fig 1: Consequence of complete deletion of *rarA* on DNA damage sensitivity**
447 **of the cell.** (A) Complete deletion of *rarA* is able to rescue the sensitivity of Δ*recF* and Δ*recO* to
448 UV and Δ*dinB* to NFZ. (B) Incorporation of Δ*rarAN406* does not rescue the sensitivity of Δ*recF*
449 and Δ*recO* to UV and Δ*dinB* to NFZ.

450

bioRxiv preprint doi: https://doi.org/10.1101/2021.11.08.467797; this version posted November 8, 2021. The copyright holder for this preprint (which was not certified by peer review) is the author/funder, who has granted bioRxiv a license to display the preprint in perpetuity. It is made available under aCC-BY 4.0 International license.

451 **Supplementary Fig 2: SOS induction is highly induced on UV exposure in cells carrying**
452 **complete deletion of *rarA* (*rarAΔN447)* from the cell.** Complete deletion of *rarA* induces SOS
453 response more than WT cell, in presence and absence of UV exposure.
454

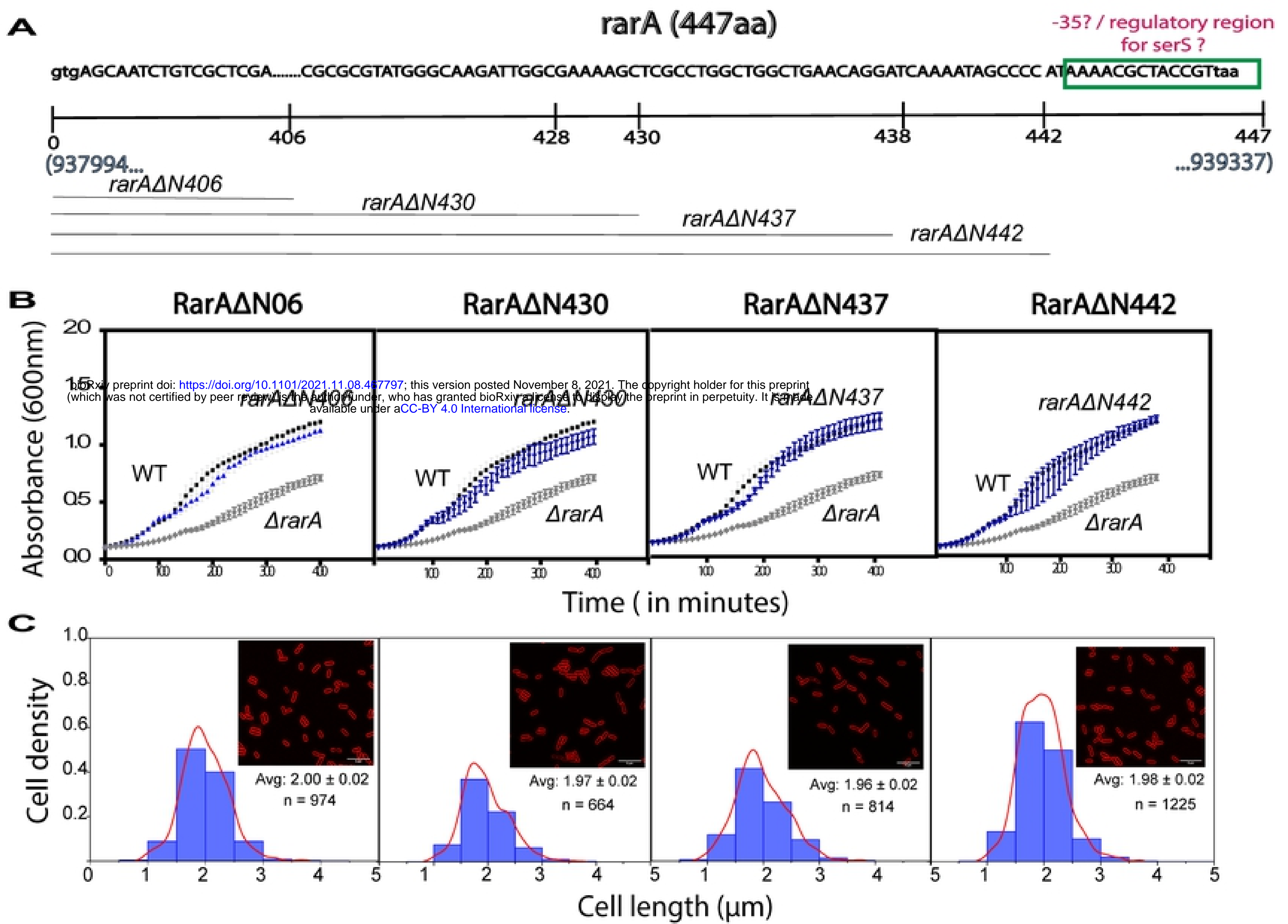

bioRxiv preprint doi: https://doi.org/10.1101/2021.11.08.467797; this version posted November 8, 2021. The copyright holder for this preprint (which was not certified by peer review) is the author/funder, who has granted bioRxiv a license to display the preprint in perpetuity. It is made available under aCC-BY 4.0 International license.

Figure 4

bioRxiv preprint doi: https://doi.org/10.1101/2021.11.08.467797; this version posted November 8, 2021. The copyright holder for this preprint (which was not certified by peer review) is the author/funder, who has granted bioRxiv a license to display the preprint in perpetuity. It is made available under aCC-BY 4.0 International license.

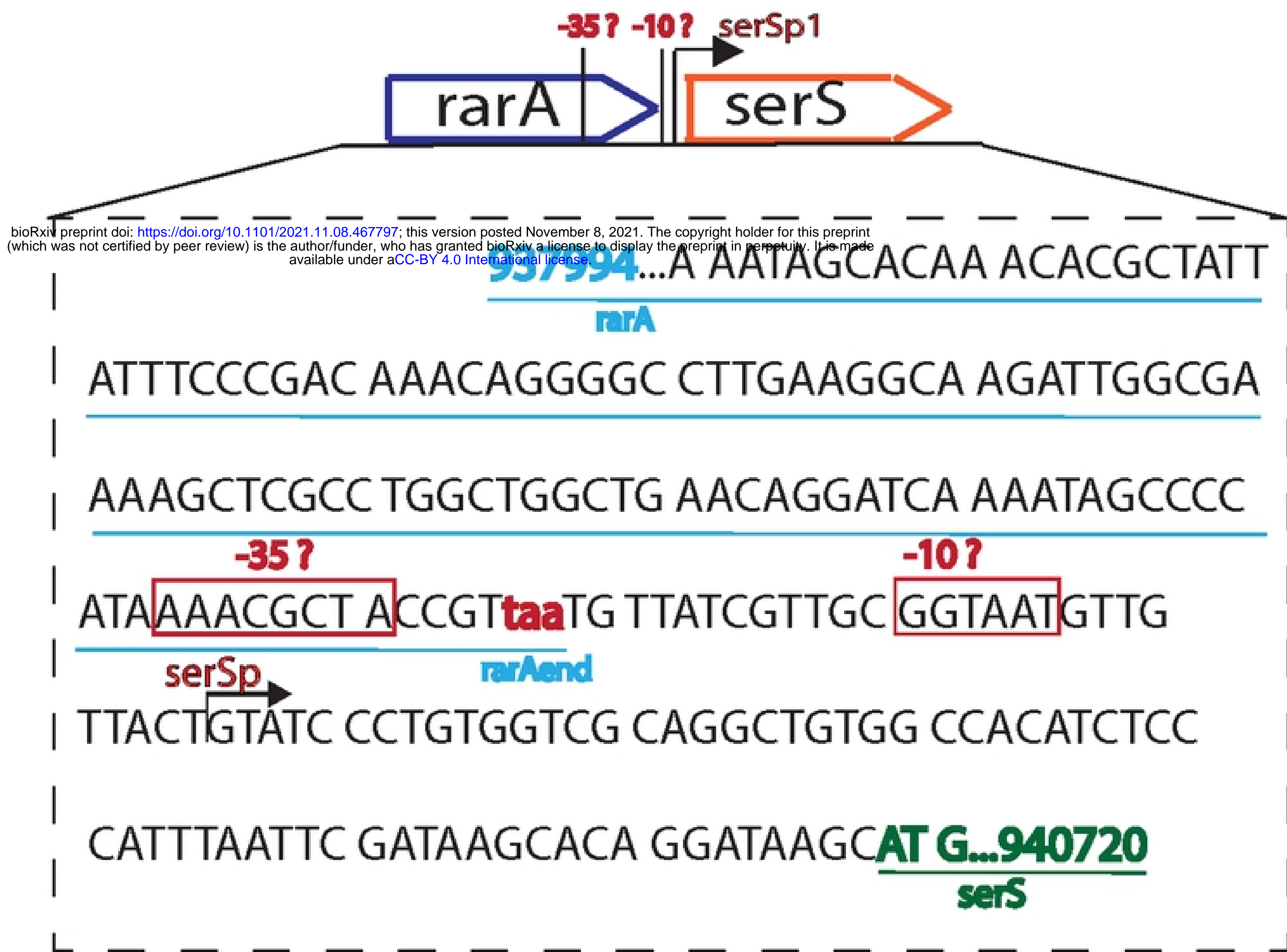

Figure 1

bioRxiv preprint doi: https://doi.org/10.1101/2021.11.08.467797; this version posted November 8, 2021. The copyright holder for this preprint (which was not certified by peer review) is the author/funder, who has granted bioRxiv a license to display the preprint in perpetuity. It is made available under aCC-BY 4.0 International license.

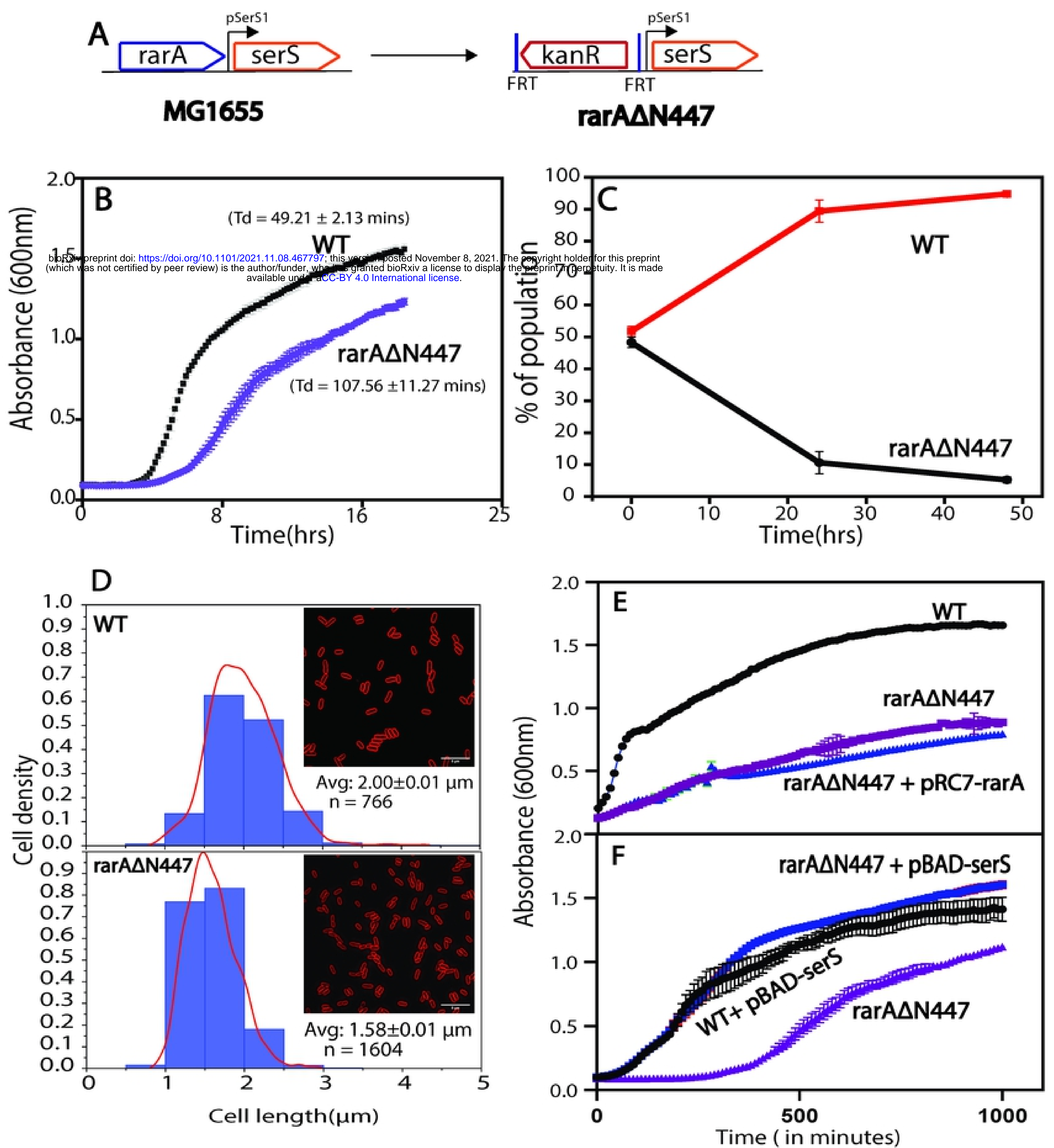

Figure 2

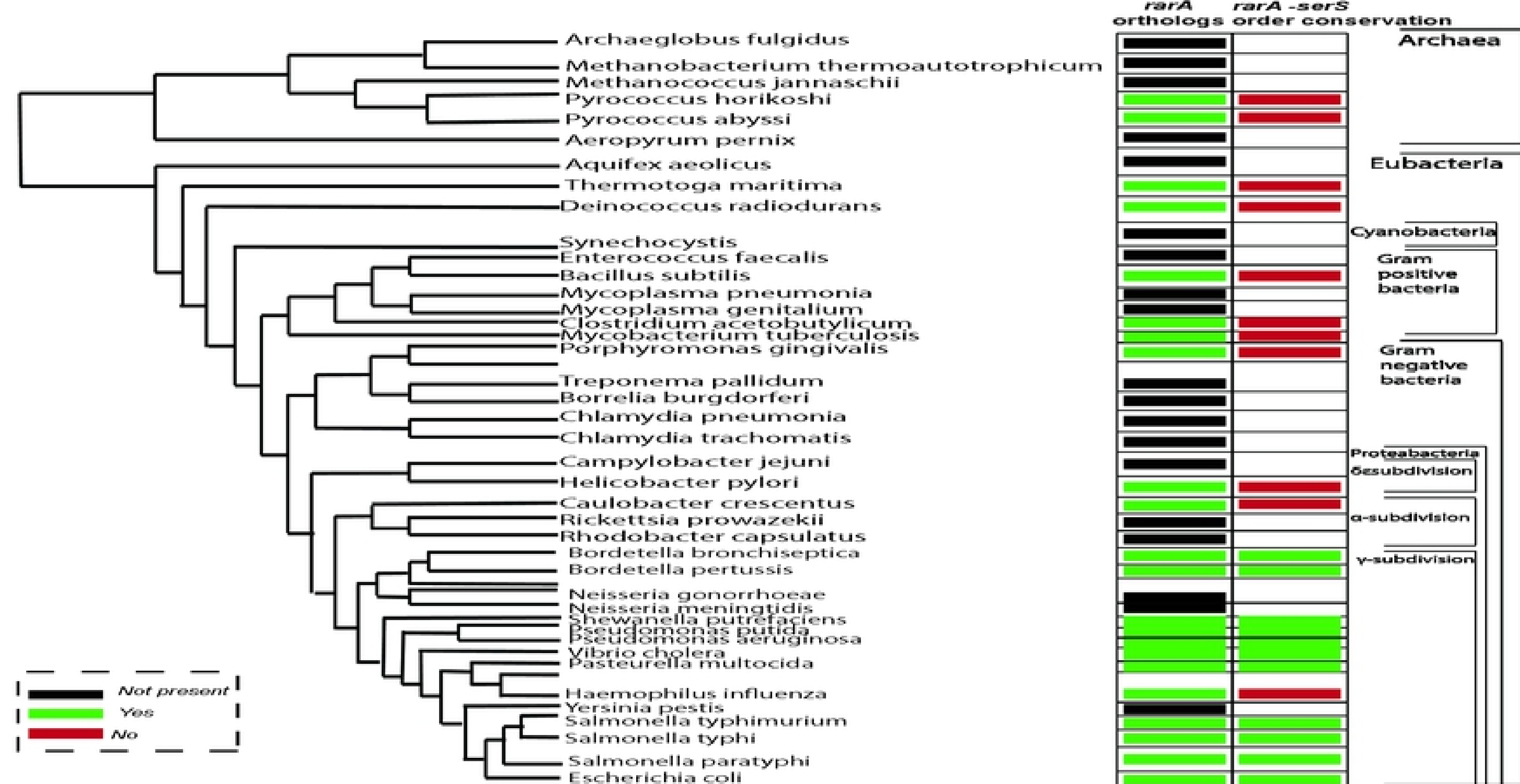

Figure 3